

**Glycolysis and pentose phosphate pathway after human  
traumatic brain injury: microdialysis studies using 1,2-<sup>13</sup>C<sub>2</sub>  
glucose**

Journal:	<i>Journal of Cerebral Blood Flow and Metabolism</i>
Manuscript ID:	JCBFM-0300-14-ORIG.R1
Manuscript Type:	Original Article
Date Submitted by the Author:	16-Aug-2014
Complete List of Authors:	Jalloh, Ibrahim; University of Cambridge, Department of Clinical Neurosciences Carpenter, Keri; University of Cambridge, Neurosurgery; University of Cambridge, Wolfson Brain Imaging Centre Grice, Peter; University of Cambridge, Department of Chemistry Howe, Duncan; University of Cambridge, Department of Chemistry Mason, Andrew; University of Cambridge, Department of Chemistry Gallagher, Clare; University of Calgary, Department of Clinical Neurosciences Helmy, Adel; University of Cambridge, Neurosurgery Murphy, Michael; University of Cambridge, MRC Mitochondrial Biology Unit Menon, D; University of Cambridge, Division of Anaesthesia; University of Cambridge, Wolfson Brain Imaging Centre Carpenter, T Adrian; University of Cambridge, Wolfson Brain Imaging Centre Pickard, John; University of Cambridge, Neurosurgery; University of Cambridge, Wolfson Brain Imaging Centre Hutchinson, Peter; University of Cambridge, Neurosurgery; University of Cambridge, Wolfson Brain Imaging Centre
Keywords:	Brain trauma, Energy Metabolism, Glucose, Lactate, Neurochemistry

Title Page

**Glycolysis and pentose phosphate pathway after human traumatic brain injury:  
microdialysis studies using 1,2-<sup>13</sup>C<sub>2</sub> glucose**

Ibrahim Jalloh MA<sup>1</sup>, Keri L.H. Carpenter PhD<sup>1,2</sup>, Peter Grice PhD<sup>3</sup>, Duncan J Howe BSc<sup>3</sup>,  
Andrew Mason BSc<sup>3</sup>, Clare N. Gallagher MD PhD<sup>1,4</sup>, Adel Helmy PhD<sup>1</sup>, Michael P. Murphy  
PhD<sup>5</sup>, David K. Menon PhD FRCP FMedSci<sup>2,6</sup>, T. Adrian Carpenter PhD<sup>2</sup>, John D. Pickard  
PhD FRCS FMedSci<sup>1,2</sup>, Peter J. Hutchinson PhD FRCS<sup>1,2</sup>

*Authors' affiliations:*

<sup>1</sup> Division of Neurosurgery, Department of Clinical Neurosciences, University of Cambridge,  
UK;

<sup>2</sup> Wolfson Brain Imaging Centre, Department of Clinical Neurosciences, University of  
Cambridge, UK;

<sup>3</sup> Department of Chemistry, University of Cambridge, UK;

<sup>4</sup> Division of Neurosurgery, Department of Clinical Neurosciences, University of Calgary,  
Canada;

<sup>5</sup> MRC Mitochondrial Biology Unit, Cambridge, UK;

<sup>6</sup> Division of Anaesthesia, Department of Medicine, University of Cambridge, UK

*Running title:* 1,2-<sup>13</sup>C<sub>2</sub> glucose metabolism in TBI

*Correspondence:*

Ibrahim Jalloh MA MRCS  
University of Cambridge, Department of Clinical Neurosciences,  
Division of Neurosurgery,  
Box 167 Cambridge Biomedical Campus  
Cambridge, CB2 0QQ  
UK

Tel: +44 1223 596497; Fax: +44 1223 216926 Email: [ij232@cam.ac.uk](mailto:ij232@cam.ac.uk)

## Funding

We gratefully acknowledge financial support as follows. Study support: Medical Research Council (Grant Nos. G0600986 ID79068 and G1002277 ID98489) and National Institute for Health Research Biomedical Research Centre, Cambridge (Neuroscience Theme; Brain Injury and Repair Theme). Authors' support: I.J. – Medical Research Council (Grant no. G1002277 ID 98489) and National Institute for Health Research Biomedical Research Centre, Cambridge; K.L.H.C. – National Institute for Health Research Biomedical Research Centre, Cambridge (Neuroscience Theme; Brain Injury and Repair Theme); C.G. – the Canadian Institute of Health Research; A.H. – Medical Research Council/ Royal College of Surgeons of England Clinical Research Training Fellowship (Grant no. G0802251) and Raymond and Beverly Sackler Fellowship; D.K.M. and J.D.P. - National Institute for Health Research Senior Investigator Awards; P.J.H. – National Institute for Health Research Professorship, Academy of Medical Sciences/Health Foundation Senior Surgical Scientist Fellowship.

## Disclosure/Conflict of Interest

J.D.P. and P.J.H. are Directors of Technicam.

Abstract

Increased ‘anaerobic’ glucose metabolism is observed after traumatic brain injury (TBI) attributed to increased glycolysis. An alternative route is the pentose phosphate pathway (PPP), which generates putatively protective and reparative molecules. To compare pathways we employed microdialysis to perfuse 1,2-<sup>13</sup>C<sub>2</sub> glucose into the brains of 15 TBI patients and macroscopically normal brain in 6 patients undergoing surgery for benign tumours, and to simultaneously collect products for NMR analysis. <sup>13</sup>C enrichment for glycolytic 2,3-<sup>13</sup>C<sub>2</sub> lactate was median 5.4% (IQR 4.6-7.5%) in TBI brain and 4.2% (2.4-4.4%) in ‘normal’ brain (p<0.01). The ratio of PPP-derived 3-<sup>13</sup>C lactate to glycolytic 2,3-<sup>13</sup>C<sub>2</sub> lactate was median 4.9% (3.6-8.2%) in TBI brain and 6.7% (6.3-8.9%) in ‘normal’ brain. An inverse relationship was seen for PPP-glycolytic lactate ratio vs. P<sub>bt</sub>O<sub>2</sub> (r=-0.5, p=0.04) in TBI brain. Thus, glycolytic lactate production was significantly greater in TBI than ‘normal’ brain. Several TBI patients exhibited PPP-lactate elevation above the ‘normal’ range. There was proportionally greater PPP-derived lactate production with decreasing P<sub>bt</sub>O<sub>2</sub>. The study raises questions about the roles of the PPP and glycolysis after TBI, and whether they can be manipulated to achieve a better outcome. This study is the first direct comparison of glycolysis and PPP in human brain.

**Keywords:** <sup>13</sup>C-labelling, glycolysis, pentose phosphate pathway, lactate, traumatic brain injury (human)

## Introduction

An increase in the proportion of glucose undergoing 'anaerobic' (non-oxygen consuming) metabolism is observed after traumatic brain injury (TBI).<sup>1-3</sup> This has been postulated to provide the energy in the form of adenosine triphosphate (ATP), produced via glycolysis, needed to restore ionic and neurochemical gradients, which become disturbed after TBI.<sup>4,5</sup> Up-regulation of the pentose phosphate pathway (PPP) has also been suggested as a possible contributor to increased anaerobic glucose metabolism after TBI, based on rat models, and indirect (arteriovenous-jugular difference) studies in human patients.<sup>6-8</sup>

Glycolysis consists of the Embden-Meyerhof pathway from glucose to pyruvate, which does not use oxygen, and generates 2 moles of ATP per mole of glucose. Pyruvate can then be metabolised via the mitochondrial tricarboxylic acid cycle (TCA) cycle coupled to mitochondrial electron transport chains, which utilise oxygen in oxidative phosphorylation. The theoretical overall yield is 36 moles of ATP per mole of glucose. Alternatively, pyruvate can be converted to lactate, which recycles NADH (reduced nicotinamide-adenine dinucleotide) to  $\text{NAD}^+$ , enabling further glucose molecules to be processed by glycolysis.

The PPP, also termed the hexose monophosphate shunt, is a biosynthetic pathway that constitutes a complex detour bypassing some of the steps of glycolysis in the metabolism of glucose. The key enzyme for the PPP, glucose-6-phosphate dehydrogenase, which is responsible for the rate-limiting step, is present in most tissues and cell types, and is regarded as a "housekeeping" enzyme.<sup>9,10</sup> The PPP does not consume or produce ATP and does not require molecular oxygen. In the early "oxidative phase" of the PPP, during which the first carbon of the glucose skeleton is lost as carbon dioxide, nicotinamide adenine dinucleotide

phosphate ( $\text{NADP}^+$ ) is converted to NADPH. The latter is a reducing agent that participates in reductive biosynthetic reactions, such as lipid and steroid synthesis, and in the production of the reduced form of glutathione and thioredoxin. Glutathione and thioredoxin are cofactors for glutathione peroxidase enzymes and peroxiredoxins respectively, both of which scavenge hydroperoxides, thereby combatting oxidative stress. Among the many intermediates of the later “non-oxidative” phase of the PPP is ribose 5-phosphate, used for nucleic acid synthesis. Hence, the proportion of glucose metabolised via the PPP is greatest in tissues with high lipid- and steroid-synthetic roles (e.g. liver and lactating mammary glands), also in cells with a high oxidative load (e.g. red blood cells), and is thought to be one of the mechanisms supporting high cell proliferation rates in cancer.<sup>10</sup> PPP activity after TBI has been postulated as playing a protective role, promoting synthesis of nucleic acids and fatty acids for tissue repair and combatting the oxidative stress that results from injured cells.<sup>6,11</sup>

Our aim was to evaluate glycolysis and the PPP as routes of glucose metabolism, directly in TBI patients’ brains. Our novel approach was to perfuse the brain using a microdialysis catheter with  $1,2\text{-}^{13}\text{C}_2$  glucose and measure the ensuing labelling patterns in lactate collected in the emerging microdialysates by analysing them using high-resolution nuclear magnetic resonance (NMR) spectroscopy. For comparison, we also carried out the same technique in ‘normal’ brain, and in muscle as a non-CNS tissue. The present study is the first direct comparison of glucose metabolism via glycolysis and PPP in human brain.

**Materials and methods**

**Patients**

The Cambridge Central Local Research Ethics Committee approved this study. Informed consent was obtained from all participants in the control ‘normal’ brain and muscle groups

and assent from the relatives of those patients who had suffered a TBI. The study was carried out in conformation with the spirit and the letter of the Declaration of Helsinki.

*TBI brain microdialysis patients:* The TBI patients were defined as those suffering cranial trauma with consistent CT scan findings and requiring invasive intracranial monitoring as part of their clinical management. Patients were managed according to local TBI-management protocols, which include endotracheal intubation, ventilation, sedation, and muscular paralysis.<sup>12</sup>

*Control 'normal' brain microdialysis patients:* Patients undergoing a craniotomy for the resection of a benign lesion whereby a microdialysis catheter could be safely placed into radiographically normal brain were selected as control subjects. The microdialysis catheter was placed via the craniotomy and tunnelled under the scalp. The control patients were awake for the duration of microdialysis perfusion.

*Muscle microdialysis patients:* Patients undergoing resections of acoustic neuromas that required thigh fat and fascia harvesting for dural closure were recruited for studying muscle, for comparison with brain. During the procedure to harvest fat and fascia a microdialysis catheter was placed under direct vision into quadriceps muscle. The muscle microdialysis subjects were under general anaesthesia for the duration of the microdialysis perfusion, which was performed at the same time of day for each patient minimising the effect of diurnal variation.

## Microdialysis technique

CMA 71 microdialysis catheters (membrane length 10 mm, nominal molecular weight cut-off 100 kDa) (M Dialysis AB, Stockholm, Sweden) were placed either via a triple lumen cranial access device (Technicam, Newton Abbot, UK) or during a craniotomy for a traumatic lesion, along with an intracranial pressure (ICP) monitor (Codman, Raynham, MA, USA) and a Licox brain tissue oxygen sensor (GMS, Kiel-Mielkendorf, Germany) into frontal lobe. For TBI patients with a diffuse injury, the right frontal region was chosen; if there was greater injury to one hemisphere rather than the other, the most injured side was chosen. The catheter was not placed within nor immediately adjacent to the lesion itself. CMA 71 catheters were used for control 'normal' brain subjects and placed via the cranial opening at the end of their neurosurgical procedure. CMA 60 catheters (membrane length 30 mm, nominal molecular weight cut-off 20 kDa) were used for muscle subjects and placed under direct vision into right quadriceps muscle following fat and fascia harvesting under general anaesthesia.

Catheters in the TBI patients and the normal brain control subjects were perfused with CNS Perfusion Fluid (M Dialysis, AB), composed of NaCl (147 mmol/L), KCl (2.7 mmol/L), CaCl<sub>2</sub> (1.2 mmol/L), and MgCl<sub>2</sub> (0.85 mmol/L) in water, supplemented with 4 mmol/L 1,2-<sup>13</sup>C<sub>2</sub> glucose (see below for details). Muscle microdialysis catheters were perfused with T1 Perfusion Fluid (M Dialysis AB), composed of NaCl (147 mmol/L), KCl (4 mmol/L), and CaCl<sub>2</sub> (2.3 mmol/L) in water, supplemented with 4 mmol/L 1,2-<sup>13</sup>C<sub>2</sub> glucose. The concentration (4 mmol/L) of <sup>13</sup>C-labelled substrate was chosen to be within the range found in brain and muscle microdialysates in unlabelled studies, to minimise perturbation.<sup>13-15</sup> 1,2-<sup>13</sup>C<sub>2</sub> glucose (isotopic enrichment 99%, chemical purity 99%) was obtained from Cambridge Isotope Laboratories, Inc (Tewksbury, MA) and was formulated in CNS perfusion fluid or T1 perfusion fluid by the Manufacturing Unit, Department of Pharmacy, Ipswich Hospital NHS Trust (Ipswich, UK), who then tested the formulations to verify purity, sterility, freedom



from endotoxins and absence of pyrogenicity, to comply with current regulations, before releasing them for use in patients. Microdialysate collection vials from the TBI patients were changed hourly and analysed at the bedside using an ISCUS analyser (M Dialysis AB) employing enzymatic colorimetric assays for glucose, lactate, pyruvate, glutamate and glycerol. Microdialysate vials from 'normal' brain and from muscle were also analysed with the ISCUS analyser at 4- and 2-hourly intervals, respectively. ICP, cerebral perfusion pressure, and brain tissue oxygen tension ( $P_{bt}O_2$ ) data from TBI patients were recorded at the bedside using ICM+ software (ICM+, University of Cambridge, UK). Microdialysate samples were stored at 4°C (or at -80°C if storage for longer than a few days was necessary) prior to NMR analysis.

### NMR analysis

Brain microdialysate samples were pooled into 24-hour periods for each individual patient. For NMR analysis, 20  $\mu$ L of deuterium oxide ( $D_2O$ ) and 50  $\mu$ L internal reference standard from a stock solution of 24.0 mmol/L 3-(trimethylsilyl)-1-propanesulfonic acid sodium salt (also termed 2,2-dimethyl-2-silapentane-5-sulfonate sodium salt or 4,4-dimethyl-4-silapentane-1-sulfonate sodium salt; DSS) (Sigma-Aldrich, Poole, Dorset, UK) in CNS perfusion fluid (M Dialysis) was added to 180  $\mu$ L of the pooled microdialysate sample. Muscle microdialysate samples were pooled into 8-hour periods. 20  $\mu$ L of  $D_2O$  and 70  $\mu$ L from a stock solution of 2.84 mmol/L DSS was added to 120  $\mu$ L of the pooled microdialysate sample. Pooled samples, after addition of  $D_2O$  and DSS, were stored at -80°. For NMR analysis, samples were transferred into 3 mm NMR tubes (Hilgenberg GmbH, Malsfeld, Germany).

$^{13}\text{C}$  and  $^1\text{H}$  NMR spectra were acquired on a Bruker Avance III HD 500 MHz spectrometer (Bruker BioSpin GmbH, Karlsruhe, Germany) with a dual  $^1\text{H}/^{13}\text{C}$  cryoprobe (CP DUL500C/H, Bruker BioSpin GmbH).  $^{13}\text{C}$  and  $^1\text{H}$  NMR spectra were acquired and processed using TopSpin software (Bruker GmbH).  $^1\text{H}$  spectra were acquired using the pulse programme noesypr1d, a 1D NOESY experiment using presaturation to suppress the water signal. Acquisition parameters included 32 scans with a d1 (relaxation delay) of 2s.  $^{13}\text{C}$  spectra were acquired using the pulse programme zgpg30, which has 30-degree flip-angle on the carbon channel, with a d1 of 3s, using 4096 (4k) scans and digitising 64K points. Power-gated broadband  $^1\text{H}$  decoupling is achieved using the 'WALTZ-16' supercycle. The receiver gain is set to a constant value in each experiment. Metabolite signals in the samples were identified by comparison of their chemical shifts (ppm, reference DSS) to values from NMR databases (BMRB - Biological Magnetic Resonance Bank, University of Wisconsin<sup>16</sup>; HMDB - Human Metabolome Database, Genome Alberta<sup>17</sup>) and to those of our own standards. To confirm the identity of peaks, in selected cases,  $^1\text{H}$ - $^{13}\text{C}$  heteronuclear single quantum correlation (HSQC) spectra were acquired on standards and patients' microdialysate samples.

To enable quantification of the signals in the  $^{13}\text{C}$  and  $^1\text{H}$  1-dimensional spectra, calibration was carried out with a series of known concentrations of standards including lactate, 3- $^{13}\text{C}$  lactate, glucose, 1,2- $^{13}\text{C}_2$  glucose, and glutamine (from Sigma-Aldrich and Cambridge Isotope Laboratories). These standards were prepared in CNS Perfusion Fluid with the same fixed concentration of  $\text{D}_2\text{O}$  and DSS as for the preparation of brain microdialysate samples (see above) as an internal standard and run under identical NMR conditions to the pooled microdialysates. Peak areas for DSS, glucose, lactate and glutamine signals identified on the  $^{13}\text{C}$  and  $^1\text{H}$  spectra were determined using combined Gaussian and Lorentzian line-shape

fitting. Peak areas relative to the DSS internal standard were used with reference to calibration curves for each signal derived from standards (see above) of known concentrations, which showed linear relationships between peak areas (ratio to DSS internal standard) and concentrations. Fractional enrichment (%) is defined as  $100 \times [^{13}\text{C}] / ([^{13}\text{C}] + [^{12}\text{C}])$  where square brackets indicate concentrations of the relevant species.  $[^{13}\text{C}]$  was determined from the  $^{13}\text{C}$  NMR spectra and  $[^{12}\text{C}]$  from the  $^1\text{H}$  spectra, using the calibration method above. The natural abundance of  $^{13}\text{C}$  is 1.1% of all carbon atoms, and  $^{13}\text{C}$  results presented for lactate (see Results section) were expressed after subtracting this natural background from the  $^{13}\text{C}$  singlet signals.  $^{13}\text{C}$  doublet signals were not background-subtracted, because the probability of two  $^{13}\text{C}$  atoms occurring next to each other naturally is 0.01%.

Interpretation of the NMR results was based on biosynthetic pathways summarised schematically in Fig. 1, which shows the lactate labelling patterns corresponding to glycolysis, which produces 2,3- $^{13}\text{C}_2$  lactate, and the PPP, which produces 3- $^{13}\text{C}$  lactate.

## Statistical Analysis

Statistical analyses performed using SPSS21 for Mac (IBM SPSS Statistics, NY) included non-parametric tests (Mann-Whitney U-test and Kruskal–Wallis one-way analysis of variance) with a preselected p-value of 0.05 for statistical significance. Results are presented as median values with the interquartile range (IQR) given in parentheses. Relationships between  $P_{\text{btO}_2}$  and the  $^{13}\text{C}$  labelling results were explored using linear regression, with Pearson's correlation coefficient  $r$  and analysis of variance (ANOVA) p values.

## Results

### Demography

Fifteen severe TBI patients (10 M, 5 F) aged 16-59 y (median 27 y) were studied using 1,2-<sup>13</sup>C<sub>2</sub> glucose (4 mmol/L) perfusion via the microdialysis catheter, with simultaneous collection of microdialysates for NMR analysis. For comparison, macroscopically normal-appearing brain was studied using the same <sup>13</sup>C-labelled microdialysis method in six patients (age range 59-73 y; 3 M, 3 F) undergoing surgery for benign brain tumours. For a non-CNS tissue comparison, thigh (quadriceps) muscle was similarly studied in four patients (age range 20-61 y; 3 M, 1 F) who underwent surgery for acoustic neuroma resection. A further seven patients (2 'normal' brain, 5 muscle) were studied by microdialysis but with plain unsupplemented perfusion fluid without 1,2-<sup>13</sup>C<sub>2</sub> glucose. The 15 TBI patients who received 1,2-<sup>13</sup>C<sub>2</sub> glucose (see above) were also studied for a baseline period with plain unsupplemented perfusion fluid (without 1,2-<sup>13</sup>C<sub>2</sub> glucose). Demographic details of all patients are presented in Supplementary Table 1.

**Baseline results compared with 1,2-<sup>13</sup>C<sub>2</sub> glucose perfusion period**

Microdialysate measurements (using the ISCUS analyser) of glucose, lactate, pyruvate, glutamate and glycerol are shown in Fig. 2. These were acquired in the 15 TBI patients during periods when the microdialysis catheter was perfused with plain unsupplemented CNS perfusion fluid and also during the 24 h period of perfusion with 1,2-<sup>13</sup>C<sub>2</sub> glucose (4 mmol/L). In 'normal' brain, ISCUS analysis was performed for two patients who received plain unsupplemented perfusion fluid and for six patients who received 24 h perfusion with 1,2-<sup>13</sup>C<sub>2</sub> glucose (4 mmol/L). In muscle, ISCUS analysis was performed for five patients who received plain unsupplemented perfusion fluid, and for four patients who received 8 h perfusion with 1,2-<sup>13</sup>C<sub>2</sub> glucose (4 mmol/L). The 8 h period for muscle was necessitated due to clinical practicalities of limb movement - microdialysis was limited to periods during the acoustic neuroma surgery.

Significant increases ( $p < 0.05$ ) in microdialysate glucose concentration (measured on the ISCUS analyser) between baseline (unsupplemented) and the  $1,2\text{-}^{13}\text{C}_2$  glucose perfusion period were seen for all three groups, as follows (medians): TBI brain (from 1.0 to 3.8 mmol/L), 'normal' brain (from 1.9 to 3.9 mmol/L) and muscle (from 2.8 to 5.3 mmol/L). The only other statistically significant, but not thought to be biologically significant, changes in ISCUS results between baseline and the  $1,2\text{-}^{13}\text{C}_2$  glucose perfusion period were for lactate/pyruvate ratio in TBI brain (from 22.2 to 24.8), for glycerol in TBI brain (from 52.0 to 69.6  $\mu\text{mol/L}$ ), and for glutamate in TBI brain (from 3.4 to 4.4  $\mu\text{mol/L}$ ) and muscle (from 7.9 to 29.7  $\mu\text{mol/L}$ ). Concentrations of  $1,2\text{-}^{13}\text{C}_2$  glucose (median and IQR) measured by  $^{13}\text{C}$  NMR in the microdialysates from TBI brain (24 h perfusion period), normal brain (24 h perfusion period) and muscle (8 h perfusion period) were respectively 2.14 (1.45-2.43), 0.93 (0.83-1.83) and 0.95 (0.59-1.25) mmol/L, with TBI significantly different from normal brain ( $p = 0.008$ ) or muscle ( $p = 0.016$ ).

Throughout the 24 h period during which the cerebral microdialysis catheter was perfused with  $1,2\text{-}^{13}\text{C}_2$  glucose, the median serum glucose concentration measured in TBI patients was 7.3 mmol/L and all values were within the range 4-12 mmol/L except for one time-point in patient 11 where glucose was 1 mmol/L. Median serum lactate concentration was 1.1 mmol/L (min 0.7, max 3.0 mmol/L). (Supplementary Fig. 1).

### **NMR results for lactate production by glycolysis and PPP, and relationship with brain tissue oxygen**

Illustrative examples of  $^{13}\text{C}$  NMR spectra of the microdialysates are shown in Fig. 3. As a result of  $1,2\text{-}^{13}\text{C}_2$  glucose perfusion, TBI brain and 'normal' brain microdialysates included a

clearly visible doublet (red stars in expansion of  $^{13}\text{C}$  spectra) for the lactate C3 methyl group, and likewise a doublet for lactate C2, indicating glycolysis-derived 2,3- $^{13}\text{C}_2$  lactate, and a smaller C3 singlet (green stars in expansion of  $^{13}\text{C}$  spectra) representing PPP-derived 3- $^{13}\text{C}$  lactate plus endogenous lactate. Qualitatively similar-appearing spectra were seen for muscle microdialysates resulting from 1,2- $^{13}\text{C}_2$  glucose perfusion. Unlabelled TBI microdialysates (with plain unsupplemented perfusion fluid) showed singlets for endogenous lactate C3 and C2 (Fig. 3).

Natural abundance of  $^{13}\text{C}$  was assumed 1.1%, and  $^{13}\text{C}$  fractional enrichment values for lactate were expressed after subtracting this naturally occurring  $^{13}\text{C}$  background from the  $^{13}\text{C}$  singlet signals. In TBI brain microdialysates,  $^{13}\text{C}$  fractional enrichment (%) in 2,3- $^{13}\text{C}_2$  lactate, indicative of glycolysis, was median 5.4% (IQR 4.6-7.5%) measured using the C3 doublet and this was significantly greater than in 'normal' brain (Fig. 4). Fractional enrichment was based on quantification of the lactate C3 doublet signal ( $^{13}\text{C}$  spectrum) to measure  $^{13}\text{C}$  at the C3 position and the lactate methyl protons (attached to C3) triplet signal ( $^1\text{H}$  spectrum) to quantify  $^{12}\text{C}$  at the C3 position. Similar  $^{13}\text{C}$  fractional enrichment to that of lactate C3 doublet was obtained using the lactate C2 doublet, as expected (Fig. 4). In muscle,  $^{13}\text{C}$  fractional enrichment in 2,3- $^{13}\text{C}_2$  lactate was lower than in TBI and 'normal' brain (Fig. 4).

Based on the lactate C3 methyl group,  $^{13}\text{C}$  fractional enrichment (%) in 3- $^{13}\text{C}$  lactate indicative of the PPP in TBI brain microdialysates was median 0.24% (IQR 0.17-0.61%) (Fig. 4) which was thus much less than the  $^{13}\text{C}$  fractional enrichment in glycolytic 2,3- $^{13}\text{C}_2$  lactate (above). The ratio in TBI brain microdialysates of PPP-derived 3- $^{13}\text{C}$  lactate to glycolytic 2,3- $^{13}\text{C}_2$  lactate was median 4.9% (IQR 3.6-8.2%) (Fig. 4). Four of the 15 TBI patients exhibited ratios of PPP-derived to glycolytic lactate (11.4, 11.5, 11.9 and 14.0%) that

were greater than the range observed in the present study in normal brain (min 5.9, max 10.4%).

In muscle, microdialysis perfusion with 1,2-<sup>13</sup>C<sub>2</sub> glucose (4 mmol/L, for 8 h) resulted in lactate C3 doublet and C2 doublet, indicating glycolytic 2,3-<sup>13</sup>C<sub>2</sub> lactate, with <sup>13</sup>C enrichment at C3 median 1.2% (range 1.0-1.4%). However, there was no <sup>13</sup>C enrichment above background natural abundance for lactate C3 singlet, so PPP production of lactate was not detected in muscle.

The concentration of 2,3-<sup>13</sup>C<sub>2</sub> lactate (indicative of glycolysis) showed a non-significant inverse trend ( $r = -0.4$ ,  $p = 0.1$ ) with brain tissue oxygen concentrations (PbtO<sub>2</sub> expressed in mm Hg) measured in the vicinity of the microdialysis catheter in TBI brain. A significant inverse correlation ( $r = -0.5$ ,  $p = 0.04$ ) was seen for the ratio of PPP-lactate to glycolytic lactate vs. PbtO<sub>2</sub> (Fig. 5). Local tissue oxygen concentration was not measured in normal brain or muscle.

Five TBI patients had a second 24 h period of 1,2-<sup>13</sup>C<sub>2</sub> glucose (4 mmol/L) microdialysis perfusion. There were no significant differences in the production of glycolytic-lactate or PPP-derived lactate between these two time periods.

## Discussion

This study has shown that 1,2-<sup>13</sup>C<sub>2</sub> glucose infusion via the microdialysis catheter results in <sup>13</sup>C-labelling in lactate (Fig. 3) in the emerging microdialysates, enabling us to compare glycolysis and PPP as routes by which lactate is derived. This is the first time this comparison has been performed directly in human brain.

**Glucose metabolism via glycolysis and the pentose phosphate pathway**

Clear evidence for glycolysis being the main route of lactate production from glucose, as expected, was seen as diagnostic doublet signals for both C3 and C2 of lactate (Fig. 3) indicating 2,3-<sup>13</sup>C<sub>2</sub> lactate, a hallmark of the pathway (Fig. 1). These doublets were seen for all patients, in TBI brain, ‘normal’ brain and muscle. This is in accord with the recognised glycolysis pathway consisting of the Embden-Meyerhof pathway from glucose to pyruvate, followed by conversion to lactate by the action of lactate dehydrogenase (Fig. 1). This <sup>13</sup>C enrichment was significantly higher in TBI brain, suggesting greater glycolytic activity, than in ‘normal’ brain and muscle. The doublet signals provide a distinctive signature that in effect avoids the issue of natural abundance <sup>13</sup>C background (1% of all carbon atoms), since the probability of two endogenous <sup>13</sup>C atoms occurring next to each other naturally is 0.01%.

The PPP loses the first carbon of 1,2-<sup>13</sup>C<sub>2</sub> glucose as carbon dioxide and thus gives rise to 3-<sup>13</sup>C lactate with a singlet signal for C3 (Fig 1). While <sup>13</sup>C singlet signals for lactate C3 were clearly visible in all patients’ microdialysates (Fig 3), these were smaller than the C3 doublet. Furthermore, it emerged that much of the C3 singlet signal intensity (peak area) was due to endogenous natural abundance <sup>13</sup>C. Small <sup>13</sup>C fractional enrichments for lactate C3 singlet above this background were seen in microdialysates from TBI brain and ‘normal’ brain, indicating PPP-derived lactate, but negligible in muscle. While there was no statistically significant difference in <sup>13</sup>C fractional enrichment for lactate C3 between ‘normal’ brain and TBI brain, the higher upper range of the latter suggests that in certain TBI individuals lactate production via the PPP is elevated above that in ‘normal’ brain. In the four TBI patients with the most elevated PPP lactate, the ratio (%) of PPP lactate to glycolytic lactate was 11.4 – 14.0%.



Our finding of increased PPP activity in some patients as a result of brain injury is supported by experimental studies. In rat models relevant to TBI, Bartnik et al. infused 1,2- $^{13}\text{C}_2$  glucose intravenously after fluid percussion injury and cortical contusion injury, and performed NMR analysis of brain tissue extracts. They found an increase in the proportion of 3- $^{13}\text{C}$  lactate (indicative of PPP) relative to 2,3- $^{13}\text{C}_2$  lactate (indicative of glycolysis), in brain-injured rats compared to control rats though with glycolysis remaining dominant.<sup>6,7</sup> In humans, Dusick et al. infused 1,2- $^{13}\text{C}_2$  glucose intravenously, with  $^{13}\text{C}$  labelling in lactate assessed by arteriovenous-jugular difference.<sup>8</sup> This study in TBI patients and controls, although it did not sample the brain directly and could only yield information on brain lactate labelling during periods when the brain was a net exporter of lactate into the vasculature, led to similar conclusions to the rat studies above.

### Significance of the PPP

The PPP is a complex biosynthetic network generating many other species besides lactate (Fig. 1) and the balance between these species can potentially shift depending on the local biology and pathology. Some PPP-derived species are potentially reparative, e.g. ribose (for nucleic acid synthesis) and NADPH (to provide reducing equivalents for fatty acid synthesis), and neuroprotective e.g. NADPH, used for producing the reduced form of glutathione and thioredoxin, which are cofactors for glutathione peroxidases and peroxiredoxins respectively, enzymes that combat oxidative stress. Accordingly, Herrero-Mendez et al. (2009) demonstrated that If one of the key regulatory enzymes of glycolysis, phosphofructokinase, is activated in neurons so that more glucose is funnelled through glycolysis at the expense of the PPP, apoptosis soon ensues due to oxidative stress.<sup>18</sup> The PPP, which does not involve molecular oxygen and does not generate ATP, can thus be regarded as sacrificing some of the

cells' supply of glucose molecules, which might otherwise have been used for ATP synthesis via glycolysis and the TCA cycle, for the sake of generating more reducing power (NADPH) and the ability to protect, repair or build cells.

NADPH is involved in many other biochemical reactions, e.g. NADPH is a cofactor for NADPH oxidase and nitric oxide synthase and if these become dysregulated, oxidative stress may ensue, with adverse consequences. Zuurbier et al. (2004) reported that inhibition of the so-called "oxidative" phase of the PPP (the early steps of the PPP responsible for NADPH production), by means of administering 6-aminonicotinamide, was cardioprotective in an ischemia-reperfusion rat heart model.<sup>19</sup> Interestingly, when Tyson et al. (2000) administered 6-aminonicotinamide to inhibit the PPP in rats in a study of brain using intravenous 2-<sup>13</sup>C glucose as the substrate, they found that despite achieving PPP inhibition, evidenced by a build-up of 6-phosphogluconate, there appeared to be a feedback effect of PPP inhibition on glycolysis, such that both pathways decreased in a constant ratio.<sup>20</sup>

**Role of brain tissue oxygen concentration in brain metabolism**

In the literature, 'hyperglycolysis' and the elevation of lactate production in the injured brain have been attributed to hypoxia and/or mitochondrial dysfunction, though the exact nature of the latter remains unclear. In a combined positron emission tomography (PET) (oxygen-15 and fluorodeoxyglucose (18F)) and microdialysis study, Vespa et al. (2005) reported that 'metabolic crisis' (defined as lactate/pyruvate ratio > 40) occurred in 7 out of 19 TBI patients studied, though only one case showed regional ischaemia judged by PET.<sup>2</sup> In a microdialysis study of 24 TBI patients in conjunction with  $P_{bt}O_2$  measurement and perfusion CT, Sala et al. (2013) concluded that the majority of lactate production was 'glycolytic' (rather than hypoxic), albeit without evidence from carbon labelling.<sup>21</sup>

In the present study, we measured  $P_{bt}O_2$  alongside the microdialysis catheter in the TBI patients, and found that there was a non-significant trend towards greater glycolytically generated 2,3- $^{13}C_2$  lactate with decreasing  $P_{bt}O_2$ . It is important to note that there were only 3 cases that could be described as hypoxic (defined as  $P_{bt}O_2 < 20$  mm Hg), and the remaining 14 data-points ranged from 22 to 43 mm Hg. Interestingly, the ratio of PPP-derived lactate to glycolytic lactate showed a significant inverse correlation with  $P_{bt}O_2$  ( $r = -0.5$ ,  $p = 0.04$ ) (Fig 5). Thus, although PPP-derived lactate was always much less than glycolytic lactate, the balance between the two appeared to shift towards the PPP with lower  $P_{bt}O_2$ . Like glycolysis, the PPP does not utilise oxygen. Studies in adult rats and in brain slices have also suggested that hypoxia increases the PPP.<sup>22</sup> In contrast, Brekke et al. (2014) found evidence for a decrease in PPP in neonatal rats after hypoxic-ischaemic injury, which the authors discussed as paradoxical.<sup>23</sup> Moreover, they postulated that the apparent inability to up-regulate the PPP in this situation might render the neonatal rats vulnerable. An analogous situation might conceivably exist in human TBI, whereby low ability to up-regulate the PPP might result in those individuals' brain tissue (either globally or locally) having increased risk of damage.

**Therapeutic up-regulation of the PPP in this context might be beneficial. Apart from hypoxia (mentioned above), a few other up-regulators of the PPP have been identified. Insulin has been shown to increase the expression of glucose-6-phosphate dehydrogenase mRNA in primary rat hepatocytes.<sup>24</sup> Dehydroascorbate, the oxidised form of vitamin C, has been shown to stimulate the activity of several PPP enzymes, increase glutathione levels and inhibit hydrogen peroxide-induced changes in mitochondrial transmembrane potential in Jurkat cells (a cancer cell line).<sup>25</sup> Although these two latter studies were not performed in brain, they nevertheless illustrate the**

principle that the PPP can be deliberately up-regulated with measurable biochemical and biological effects.

**Significance of lactate in the brain**

Lactate has been conventionally regarded as a waste product of glucose metabolism, though a more recent idea is that it can act as a brain fuel - neurons take up lactate (produced from glucose by glia), metabolise lactate to pyruvate, which is transported into the mitochondria and converted to acetyl CoA, which enters the tricarboxylic acid (TCA) cycle. This has become known as the astrocyte-neuron lactate shuttle hypothesis.<sup>26</sup> Animal studies have provided evidence for brain utilisation of intravenously administered 3-<sup>13</sup>C lactate via the TCA cycle.<sup>27</sup> In human brain, direct evidence for utilisation of lactate was first obtained in a cerebral microdialysis study in TBI patients.<sup>28</sup> In the latter study, administration of 3-<sup>13</sup>C lactate via the microdialysis catheter, and simultaneous collection of the emerging microdialysates, with <sup>13</sup>C NMR analysis, revealed <sup>13</sup>C labelling in glutamine consistent with lactate utilisation via the TCA cycle.<sup>28</sup> Recently, an intravenous lactate supplementation study in TBI patients revealed evidence for a beneficial effect judged by surrogate endpoints.<sup>29</sup> Studies of brain microdialysates (without supplementation) in 223 patients show a statistical association between high extracellular lactate and unfavourable outcome.<sup>30</sup> Taken together, available evidence suggests that where neurons are too damaged to utilise the lactate produced from glucose by astrocytes, i.e. uncoupling of neuronal and glial metabolism, high extracellular levels of lactate would accumulate, explaining one potential mechanism behind the association between high extracellular lactate and poor outcome.

**Fate of lactate**

Regarding the possible fate of labelled lactate produced from 1,2- $^{13}\text{C}_2$  glucose, a likely scenario is that some of the labelled lactate is processed via the TCA cycle, and some of it exported into the bloodstream. Since we were micro-dosing the brain with 1,2- $^{13}\text{C}_2$  glucose locally via the microdialysis catheter, it seemed highly unlikely that any of the ensuing doubly labelled lactate would have been detectable in the bloodstream given the inevitable dilution both with endogenous unlabelled lactate and with the volume of blood, so  $^{13}\text{C}$  NMR analyses of blood were not performed.

Previously, using 3- $^{13}\text{C}$  lactate as the substrate, we detected singly labelled glutamine (and/or glutamate) in TBI brain microdialysates, indicating utilisation of lactate via the TCA cycle.<sup>28</sup> In the present study, if 2,3- $^{13}\text{C}_2$  lactate (produced from the substrate 1,2- $^{13}\text{C}_2$  glucose) entered the TCA cycle in brain cells, this would in theory have resulted in doublets in the  $^{13}\text{C}$  NMR spectra, due to 4,5- $^{13}\text{C}_2$  glutamine and 2,3- $^{13}\text{C}_2$  glutamine (and/or glutamate in each case) on the first turn of the cycle, and, on the second turn, doublets due to 1,2- $^{13}\text{C}_2$  glutamine and a singlet due to 3- $^{13}\text{C}$  glutamine.<sup>23,31</sup> Experimental models of brain injury in rodents, using 1,2- $^{13}\text{C}_2$  glucose as substrate, with analysis of brain tissue extracts representing total intracellular and extracellular molecules, confirm double labelling in glutamate and glutamine.<sup>6,7,31</sup> In our present study, small singlet signals, but not doublets, corresponding to glutamine were seen in the  $^{13}\text{C}$  NMR spectra of some of the microdialysates from 'normal' brain (4/6 patients) and TBI (2/15 patients), verified by 2-D NMR methods, including  $^1\text{H}$ - $^{13}\text{C}$  HSQC (Supplementary Fig. 2). In theory, pyruvate cycling,<sup>32</sup> which breaks the  $^{13}\text{C}$ - $^{13}\text{C}$  bond might explain the glutamine singlets. Also, in theory, PPP-derived 3- $^{13}\text{C}$  lactate might enter the TCA cycle forming singly-labelled glutamine (and/or glutamate), although accompanied by doubly-labelled glutamine from glycolytic 2,3- $^{13}\text{C}_2$  lactate, as found in vitro by Brekke et al.

(2012).<sup>33</sup> However, in the present study, quantification of the small glutamine singlets revealed no significant <sup>13</sup>C enrichment above natural abundance.

Microdialysis only samples the extracellular compartment and therefore cannot measure the intracellular distribution of <sup>13</sup>C. Even so, our <sup>13</sup>C-labelled microdialysis method provides a useful means for measuring ‘early’ glucose metabolism (glycolysis and PPP) as sufficient labelled lactate is exported into the extracellular compartment to allow detection. However, in the subsequent metabolism of lactate, the downstream dilution of <sup>13</sup>C label with endogenous unlabelled intermediates probably explains why we did not observe significant <sup>13</sup>C enrichment of extracellular metabolites derived from the TCA cycle. In our previous study, when 3-<sup>13</sup>C lactate (4 mmol/L) or 2-<sup>13</sup>C acetate (4 mmol/L) was perfused via the microdialysis catheter in TBI brain, labelling in glutamine consistent with TCA cycle was seen in the emerging microdialysates.<sup>28</sup> However, in the same study, perfusion with 1-<sup>13</sup>C glucose (2 mmol/L) resulted in negligible labelling in glutamine, consistent with the present study.

**Strengths and limitations**

This <sup>13</sup>C-labelled microdialysis method, performed in parallel with local brain tissue oxygen measurement, provides a method of measuring glycolytic conversion of glucose into lactate and at the same time distinguishing hypoxic from non-hypoxic glycolysis, as well as evaluating the contribution of the PPP. Even though our evidence indicates a minor PPP-derived lactate (3-<sup>13</sup>C lactate), it must be remembered that the PPP is a complex network of biosynthetic reactions (Fig. 1) and it is conceivable that if heavy recycling is operating within the PPP, less lactate might emerge, though with elevated production of NADPH and intermediates utilised in neuroprotection and repair of cells.

The strategy of double labelling (using 1,2- $^{13}\text{C}_2$  glucose as substrate) provides a characteristic signature that appears in glycolytic lactate (2,3- $^{13}\text{C}_2$  lactate) showing that the  $^{13}\text{C}$ - $^{13}\text{C}$  covalent bond stays intact. Moreover the doublet signal is essentially free from endogenous lactate as the probability of two  $^{13}\text{C}$  atoms being adjacent to each other naturally is 0.01%. Like all cerebral microdialysis the  $^{13}\text{C}$ -labelled microdialysis method is invasive, so is only suitable for severe TBI patients or those requiring brain surgery (e.g. for tumours), and it is a focal technique.

This  $^{13}\text{C}$ -labelling method has the potential to be a useful adjunct to existing methodologies of PET and unlabelled microdialysis in monitoring and studying TBI patients. The  $^{13}\text{C}$ -labelled microdialysis method does not involve disruption of the patient's standard medical care on the neurocritical care unit, and does not involve radioactivity or moving the patient to a scanner. The 1,2- $^{13}\text{C}_2$  glucose microdialysis method is reasonably inexpensive and convenient to perform, since 1 or 2 g of the labelled material are enough to formulate enough perfusion fluid for multiple patients, and the formulation can be stored in individual sterile ready-to-use sealed glass vials in a refrigerator. The concentration (4 mmol/L) of 1,2- $^{13}\text{C}_2$  glucose administered via microdialysis locally into brain corresponds to the upper end of the 'normal' range found in brain ECF.<sup>13</sup> While conventional microdialysis performed with unsupplemented perfusion fluid allows us to measure endogenous extracellular lactate, the unsupplemented method cannot inherently distinguish between 'old' lactate and recently synthesised lactate. An advantage of the 1,2- $^{13}\text{C}_2$  glucose microdialysis method is that enables measurement of labelled lactate production within a known timeframe – at present this is 24h, because of current practical NMR considerations (see below).

A current limitation to our  $^{13}\text{C}$ -labelled microdialysis method is the amount of material necessary for performing NMR analysis. We have combined brain microdialysates for a 24h period for each patient, to facilitate  $^{13}\text{C}$  NMR spectroscopy within a convenient acquisition time on the spectrometer. Our Bruker Avance 500 MHz spectrometer is equipped with a cryoprobe, as used in the present study and in our previous study,<sup>28</sup> which is more sensitive than non-cryo probe technology. Even so, the practical limit with our present equipment limits us in terms of how short a timeframe we can analyse in terms of microdialysis perfusion. Having better time-resolution for the microdialysis labelling results would be useful from a biochemical perspective allowing time-course evaluation. 1,2- $^{13}\text{C}_2$  glucose microdialysis may have future potential for metabolic kinetic modelling of local glucose consumption rates and glycolytic- and PPP- production rates of lactate. Commercially available NMR micro-cryoprobes, which take smaller volumes, may be useful in future. Analysis by mass spectrometry might also be useful in future, enabling smaller volumes to be analysed, though at the expense of at least some of the detailed information on precise intra-molecular position of label.

**Conclusion**

Here we have shown that  $^{13}\text{C}$  labelled microdialysis can be used to interrogate glucose metabolism via glycolysis and the PPP. The major pathway, glycolytic lactate production, was significantly greater in TBI brain than in normal brain. The minor pathway, PPP-derived lactate production, was statistically not significantly different in TBI brain than in normal brain. However, several of the TBI individuals showed PPP-derived lactate elevation above the range observed in normal brain. There was a shift in glucose metabolism from glycolysis to PPP with decreasing brain tissue oxygen concentrations. The findings raise interesting questions about the roles of the PPP and glycolysis after TBI, and whether they can be



manipulated to enhance the potentially reparative and antioxidant role of the PPP and achieve a better outcome for the patient. The  $^{13}\text{C}$  methodology developed here provides a means of distinguishing recently synthesised lactate and its biosynthetic origin, and at the same time measuring local oxygen tension alongside.  $^{13}\text{C}$ -labelled microdialysis with 1,2- $^{13}\text{C}_2$  glucose as substrate may thus find a methodological role in studies of hyperoxia or strategies to optimise perfusion and mitochondrial function. This is the first time that a comparison between glycolysis and the PPP has been carried out directly in human brain.

### Acknowledgments

We thank Mr. R. Kirolos, Mr. R. Macfarlane and Mr. R. Mannion for assistance in placing microdialysis catheters into the control subjects. We thank Dr. R.J. Shannon for assistance with microdialysate analysis. We thank Mr. John Harwood (Ipswich Hospital NHS Trust) for supervising the formulation of the  $^{13}\text{C}$  substrate.

### Disclosure/Conflict of Interest

J.D.P. and P.J.H. are Directors of Technicam.

### Supplementary Material

Supplementary information is available at the Journal of Cerebral Blood Flow & Metabolism website – [www.nature.com/jcbfm](http://www.nature.com/jcbfm)

References

1. Bergsneider M, Hovda DA, Shalmon E, Kelly DF, Vespa PM, Martin NA, et al. Cerebral hyperglycolysis following severe traumatic brain injury in humans: a positron emission tomography study. *J Neurosurg* 1997;86:241–51.
2. Vespa P, Bergsneider M, Hattori N, Wu H-M, Huang S-C, Martin NA, et al. Metabolic crisis without brain ischemia is common after traumatic brain injury: a combined microdialysis and positron emission tomography study. *J Cereb Blood Flow Metab* 2005;25:763–74.
3. Wu H-M, Huang S-C, Vespa P, Hovda DA, Bergsneider M. Redefining the pericontusional penumbra following traumatic brain injury: evidence of deteriorating metabolic derangements based on positron emission tomography. *J Neurotrauma* 2013;30:352–60.
4. Katayama Y, Becker DP, Tamura T, Hovda DA. Massive increases in extracellular potassium and the indiscriminate release of glutamate following concussive brain injury. *J Neurosurg* 1990;73:889–900.
5. Kawamata T, Katayama Y, Hovda DA, Yoshino A, Becker DP. Administration of Excitatory Amino Acid Antagonists via Microdialysis Attenuates the Increase in Glucose Utilization Seen Following Concussive Brain Injury. *J Cereb Blood Flow Metab* 1992;12:12–24.
6. Bartnik BL, Sutton RL, Fukushima M, Harris NG, Hovda DA, Lee SM. Upregulation of pentose phosphate pathway and preservation of tricarboxylic acid cycle flux after experimental brain injury. *J Neurotrauma* 2005;22:1052–65.
7. Bartnik BL, Lee SM, Hovda DA, Sutton RL. The fate of glucose during the period of decreased metabolism after fluid percussion injury: a <sup>13</sup>C NMR study. *J Neurotrauma* 2007;24:1079–92.
8. Dusick JR, Glenn TC, Lee WNP, Vespa PM, Kelly DF, Lee SM, et al. Increased pentose phosphate pathway flux after clinical traumatic brain injury: a [1,2-<sup>13</sup>C<sub>2</sub>]glucose labeling study in humans. *J Cereb Blood Flow Metab* 2007;27:1593–602.
9. Pandolfi P, Sonati F, Rivi R, Mason P, Grosveld F, Luzzatto L. Targeted disruption of the housekeeping gene encoding glucose 6-phosphate dehydrogenase (G6PD): G6PD is dispensable for pentose synthesis but essential for defense against oxidative stress. *The EMBO Journal* 1995;14:5209.
10. Riganti C, Gazzano E, Polimeni M, Aldieri E, Ghigo D. The pentose phosphate pathway: An antioxidant defense and a crossroad in tumor cell fate. *Free Radical Biology and Medicine* 2012;53:421–36.
11. Ben-Yoseph O, Boxer PA, Ross BD. Assessment of the Role of the Glutathione and Pentose Phosphate Pathways in the Protection of Primary Cerebrocortical Cultures from Oxidative Stress. *J Neurochem* 1996;66:2329–37.

12. Helmy A, Vizcaychipi M, Gupta AK. Traumatic brain injury: intensive care management. *British Journal of Anaesthesia* 2007;99:32–42.
13. Reinstrup P, Ståhl N, Mellergård P, Uski T, Ungerstedt U, Nordström C. Intracerebral microdialysis in clinical practice: baseline values for chemical markers during wakefulness, anesthesia, and neurosurgery. *Neurosurgery* 2000;47:701–9–discussion709–10.
14. Rosdahl H, Ungerstedt U, Jorfeldt L. Interstitial glucose and lactate balance in human skeletal muscle and adipose tissue studied by microdialysis. *J Physiol* 1993;471:637–57.
15. Schulz MK, Wang LP, Tange M, Bjerre P. Cerebral microdialysis monitoring: determination of normal and ischemic cerebral metabolisms in patients with aneurysmal subarachnoid hemorrhage. *J Neurosurg* 2000;93:808–14.
16. Ulrich EL, Akutsu H, Doreleijers JF, Harano Y, Ioannidis YE, Lin J, et al. BioMagResBank [Internet]. *Nucleic Acids Res* 2007 [cited 2013 Oct 11];36:D402–8. Available from: <http://www.bmrb.wisc.edu>
17. Wishart DS, Tzur D, Knox C, Eisner R, Guo AC, Young N, et al. HMDB: the Human Metabolome Database [Internet]. *Nucleic Acids Res* 2007 [cited 2013 Oct 11];35:D521–6. Available from: <http://www.hmdb.ca>
18. Herrero-Mendez A, Almeida A, Fernández E, Maestre C, Moncada S, Bolaños JP. The bioenergetic and antioxidant status of neurons is controlled by continuous degradation of a key glycolytic enzyme by APC/C–Cdh1. *Nat Cell Biol* 2009;11:747–52.
19. Zuurbier CJ, Eerbeek O, Goedhart PT, Struys EA, Verhoeven NM, Jakobs C, et al. Inhibition of the pentose phosphate pathway decreases ischemia-reperfusion-induced creatine kinase release in the heart. *Cardiovasc Res* 2004;62:145–53.
20. Tyson RL, Perron J, Sutherland GR. 6-Aminonicotinamide inhibition of the pentose phosphate pathway in rat neocortex. *Neuroreport* 2000;11:1845–8.
21. Sala N, Suys T, Zerlauth J-B, Bouzat P, Messerer M, Bloch J, et al. Cerebral extracellular lactate increase is predominantly nonischemic in patients with severe traumatic brain injury. *J Cereb Blood Flow Metab* 2013;33:1815–22.
22. Domańska-Janik K. Hexose monophosphate pathway activity in normal and hypoxic rat brain. *Resuscitation* 1988;16:79–90.
23. Brekke EMF, Morken TS, Widerøe M, Håberg AK, Brubakk A-M, Sonnewald U. The pentose phosphate pathway and pyruvate carboxylation after neonatal hypoxic-ischemic brain injury. *J Cereb Blood Flow Metab* 2014;34:724–34.
24. Talukdar I, Szeszel-Fedorowicz W, Salati LM. Arachidonic acid inhibits the insulin induction of glucose-6-phosphate dehydrogenase via p38 MAP kinase. *J Biol Chem* 2005;280:40660–7.
25. Puskas F, Gergely P, Banki K, Perl A. Stimulation of the pentose phosphate pathway and glutathione levels by dehydroascorbate, the oxidized form of vitamin C. *FASEB J*

- 2000;14:1352–61.
26. Pellerin L, Magistretti PJ. Glutamate uptake into astrocytes stimulates aerobic glycolysis: a mechanism coupling neuronal activity to glucose utilization. *Proc Natl Acad Sci USA* 1994;91:10625–9.
27. Tyson RL, Gallagher CN, Sutherland GR. <sup>13</sup>C-Labeled substrates and the cerebral metabolic compartmentalization of acetate and lactate. *Brain Res* 2003;992:43–52.
28. Gallagher CN, Carpenter KLH, Grice P, Howe DJ, Mason A, Timofeev I, et al. The human brain utilizes lactate via the tricarboxylic acid cycle: a <sup>13</sup>C-labelled microdialysis and high-resolution nuclear magnetic resonance study. *Brain* 2009;132:2839–49.
29. Bouzat P, Sala N, Suys T, Zerlauth J-B, Marques-Vidal P, Feihl F, et al. Cerebral metabolic effects of exogenous lactate supplementation on the injured human brain. *Intensive Care Med* 2014;40:412–21.
30. Timofeev I, Carpenter KLH, Nortje J, Al-Rawi PG, O'Connell MT, Czosnyka M, et al. Cerebral extracellular chemistry and outcome following traumatic brain injury: a microdialysis study of 223 patients. *Brain* 2011;134:484–94.
31. Bartnik BL, Hovda DA, Lee PWN. Glucose metabolism after traumatic brain injury: estimation of pyruvate carboxylase and pyruvate dehydrogenase flux by mass isotopomer analysis. *J Neurotrauma* 2007;24:181–94.
32. Cruz F, Cerdán S. Quantitative <sup>13</sup>C NMR studies of metabolic compartmentation in the adult mammalian brain. *NMR Biomed* 1999;12:451–62.
33. Brekke EMF, Walls AB, Schousboe A, Waagepetersen HS, Sonnewald U. Quantitative importance of the pentose phosphate pathway determined by incorporation of <sup>13</sup>C from [2-<sup>13</sup>C]- and [3-<sup>13</sup>C]glucose into TCA cycle intermediates and neurotransmitter amino acids in functionally intact neurons. *J Cereb Blood Flow Metab* 2012;32:1788–99.
34. Carpenter KLH, Jalloh I, Gallagher CN, Grice P, Howe DJ, Mason A, et al. (<sup>13</sup>C)-labelled microdialysis studies of cerebral metabolism in TBI patients. *Eur J Pharm Sci* 2014;57:87–97.

## Titles and legends to figures

**Fig. 1.** Simplified schematic of steps in glycolysis and the pentose phosphate pathway (PPP), showing  $^{13}\text{C}$  labelling patterns resulting from  $1,2\text{-}^{13}\text{C}_2$  glucose substrate. Red fills indicate  $^{13}\text{C}$  atoms. Abbreviations: Glc-6-P, glucose-6-phosphate; 6PGL, 6-phosphogluconolactone; F6P, fructose-6-phosphate; G3P, glyceraldehyde-3-phosphate; PYR, pyruvate. Figure originally published in Eur J Pharm Sci 2014; 57: 87-97 (Carpenter KLH et al.) under a Creative Commons Attribution License.<sup>34</sup>

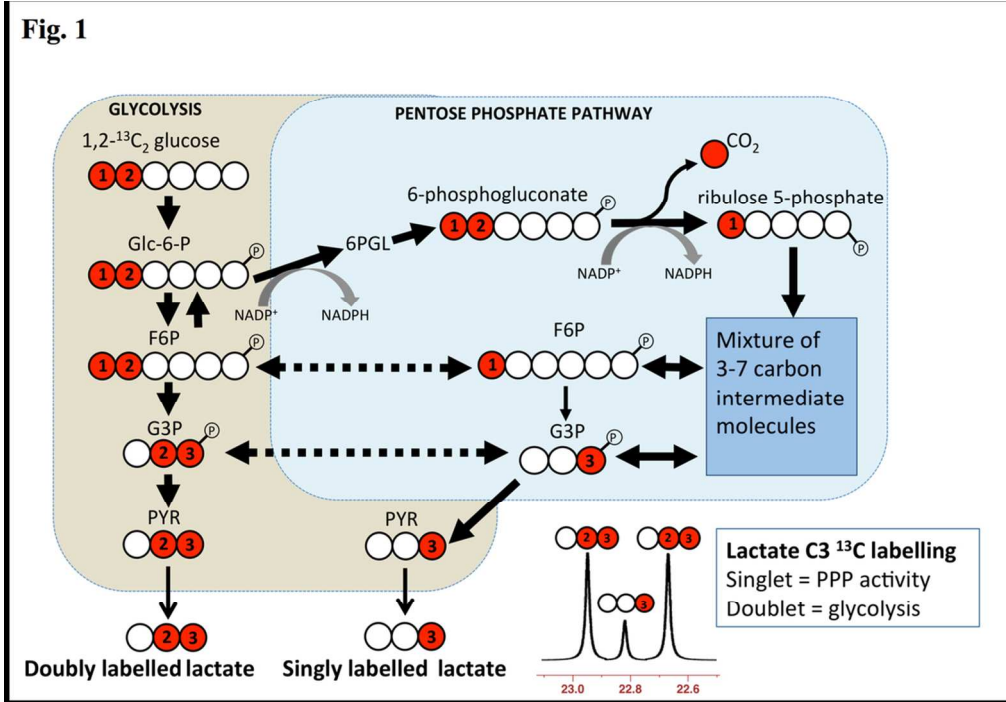
**Fig. 2.** ISCUS clinical microdialysis analyser measurements: at baseline (light grey bars) with plain unsupplemented perfusion fluid and during 24 h perfusion (brain: TBI or normal) or 8 h perfusion (muscle) with  $1,2\text{-}^{13}\text{C}_2$  glucose (4 mmol/L) (dark grey bars). LPR is the lactate/pyruvate ratio. \* $p < 0.05$  (Mann-Whitney) for baseline vs. perfusion with  $1,2\text{-}^{13}\text{C}_2$  glucose. Box and whisker plots represent pooled data. Numbers of patients with baseline (unsupplemented) measurements were 15 TBI, 2 'normal' brain and 5 muscle. Numbers of patients who received  $1,2\text{-}^{13}\text{C}_2$  glucose were 15 TBI, 6 'normal' brain and 4 muscle. 'Normal' brain was macroscopically normal-appearing brain in patients who underwent surgery for benign brain tumours. Muscle was leg quadriceps in patients undergoing acoustic neuroma resection surgery.

**Fig. 3.** Illustrative examples of  $^{13}\text{C}$  NMR spectra for microdialysates from patients who received perfusion with  $1,2\text{-}^{13}\text{C}_2$  glucose (4 mmol/L): TBI brain (uppermost two spectra, 24 h perfusion), 'normal' brain (third spectrum, 24 h perfusion), and muscle (bottom spectrum, 8 h perfusion). An example of brain microdialysate from an unlabelled TBI patient with plain (unsupplemented) perfusion fluid is shown for comparison (fourth spectrum). Examples of expansion of the lactate C3 signal are shown for TBI brain and 'normal' brain. Red stars

indicate lactate C3 doublet (due to glycolytic 2,3-<sup>13</sup>C<sub>2</sub> lactate) and green stars indicate C3 singlet (due to pentose phosphate pathway-derived 3-<sup>13</sup>C lactate plus endogenous lactate). Abbreviations: glucose (Glc), lactate (Lac), 4,4-dimethyl-4-silapentane-1-sulfonate sodium salt (DSS, the internal reference standard). Spectra were run from -20 ppm to +250 ppm. The main reference DSS signal at 0 ppm is not shown in the range illustrated.

**Fig. 4.** Microdialysate NMR measurements of <sup>13</sup>C labelling: results from perfusion for 24 h (brain: TBI or ‘normal’) or 8 h perfusion (muscle) with 1,2-<sup>13</sup>C<sub>2</sub> glucose (4 mmol/L). Red asterisks denote  $p < 0.01$  for TBI vs. ‘normal’ brain (Mann-Whitney); other comparisons asterisked in black denote  $p < 0.05$ . Individual data-points are shown by x symbols. Number of patients: 15 TBI, 6 ‘normal’ brain, 4 muscle.

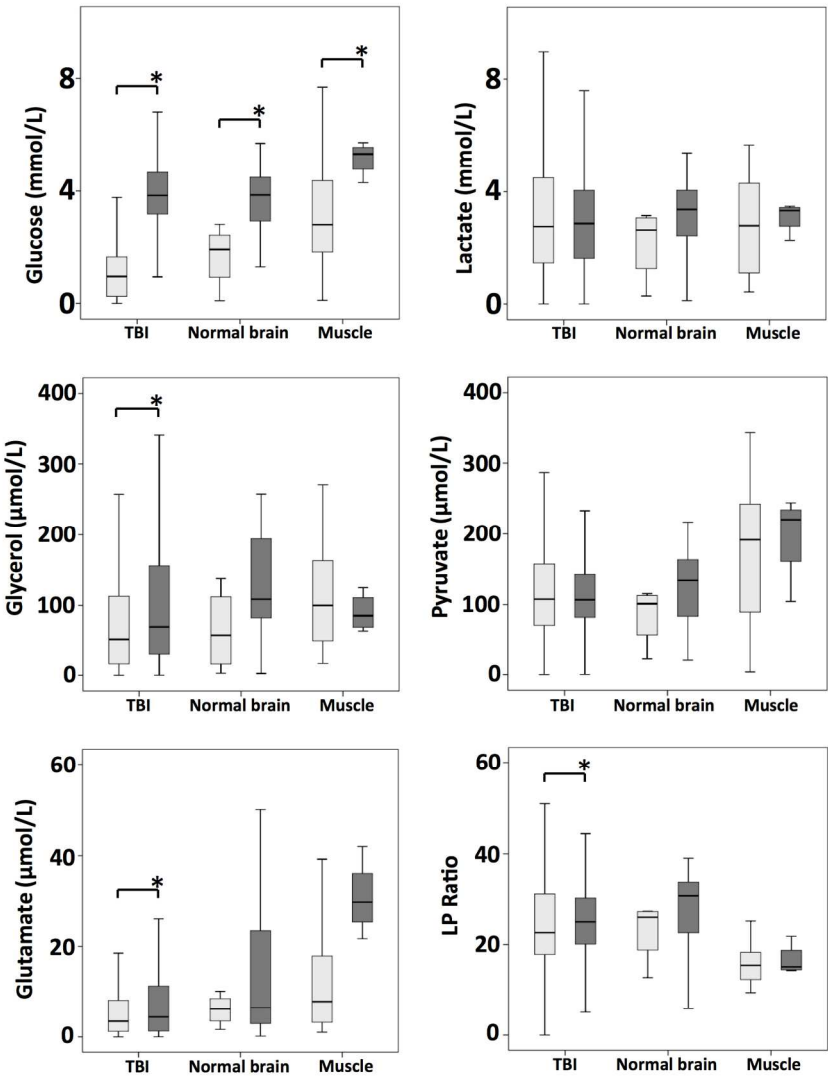
**Fig. 5.** Relationships in TBI brain for glycolytic lactate and pentose phosphate pathway (PPP)-derived lactate vs.  $P_{bt}O_2$ . Concentrations of glycolytic 2,3-<sup>13</sup>C<sub>2</sub> lactate (upper panel) and PPP-derived 3-<sup>13</sup>C lactate (middle panel) plotted vs.  $P_{bt}O_2$ . Lower panel: ratio (%) of PPP-derived 3-<sup>13</sup>C lactate to glycolytic 2,3-<sup>13</sup>C<sub>2</sub> lactate, plotted vs.  $P_{bt}O_2$ . Each data-point represents the results of NMR analysis of the combined contents of 24 x 1 h of microdialysate collection vials from one microdialysis catheter, plotted against the corresponding  $P_{bt}O_2$  concentration expressed in mm Hg, measured using a Licox oxygen probe placed alongside the microdialysis catheter in the brain. Lines are fitted by linear regression (statistics shown are Pearson’s correlation coefficient  $r$  and ANOVA  $p$  value). Data are from 13 TBI patients. Four of these 13 had a second period of monitoring, making 17 data-points in total for each correlation.



52x36mm (600 x 600 DPI)



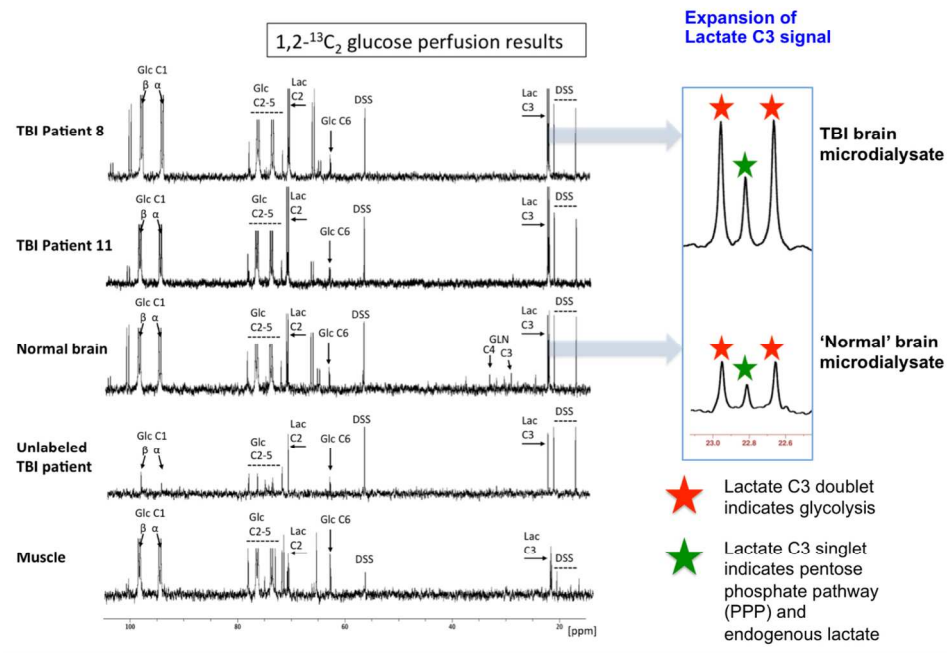
Fig. 2



92x123mm (600 x 600 DPI)

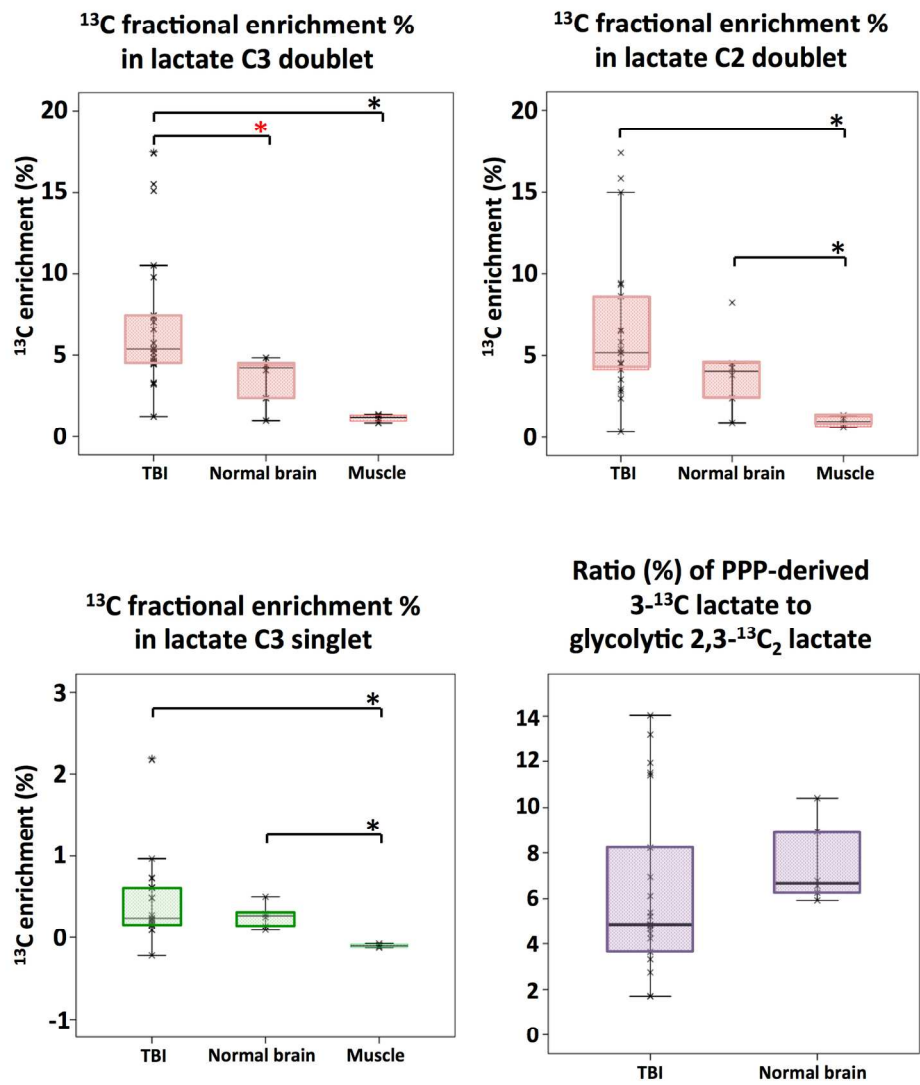


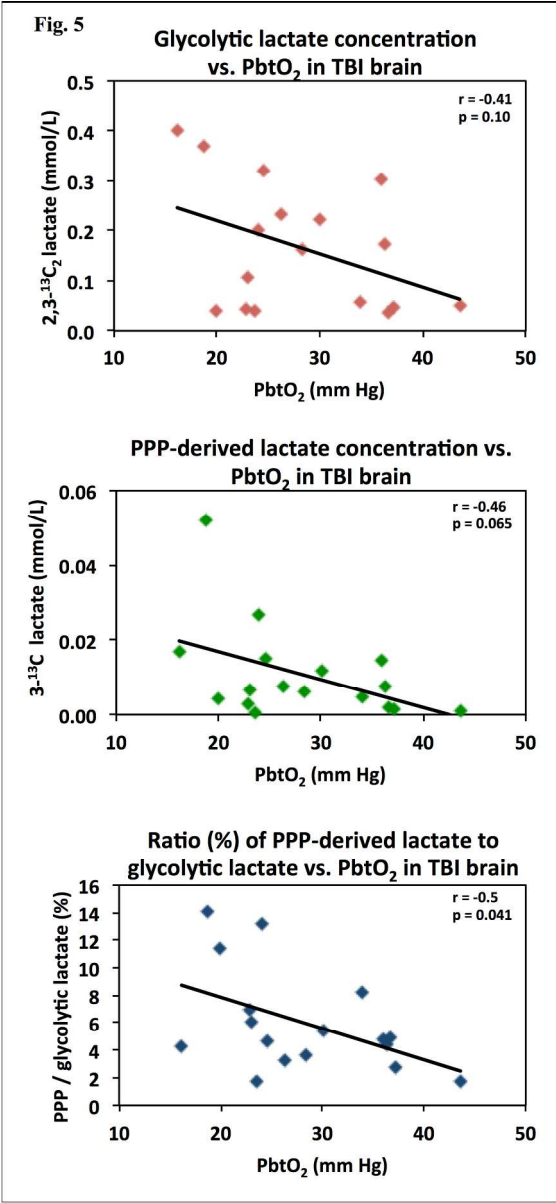
Fig. 3



69x50mm (600 x 600 DPI)

Fig. 4





120x260mm (600 x 600 DPI)